Draft version June 5, 2023
Typeset using LaTeX default style in AASTeX631

Period Analysis of W UMa Binary Systems

Thomas Sweeney, Matt Ketkaroonkul, Mikhail Mazukabzov, Peter Zhou[1]

[1] *University of Washington*

(Received June 5, 2023)

ABSTRACT

OU Ser, CC Com, and TZ Boo are W UMa eclipsing contact binaries with known periods ranging from 0.221 to 0.298 days. Photometric data of each of these systems was collected using the ARCSAT telescope at Apache Point Observatory. Fifteen second exposures in the V band were taken throughout a night to in an attempt to measure the period of each system. Each image was reduced by removing the bias, dark current, and flat field. Then, aperture photometry with local background subtraction was used to determine the flux for each image taken. Using quadratic fitting, light curves for TZ Boo and CC Com were successfully made, having periods of 0.5129 and 0.2950 days respectively. The large error in period calculation is mainly due to a small data set limiting the available fitting options.

1. INTRODUCTION

Binary star systems are systems with two stars in orbit around one another. Binary stars offer a unique opportunity for studying stellar properties. Through determining their periods, other physical properties such as the individual masses of the stars can be determined. (Carroll & Ostlie 2017) Through observing interactions between the two stars, more can be learned about each individually. An essential first step in making these measurements, is determining an accurate period for each system.

There are many types of binary systems. The largest classification of binary systems is detached, semi-detached, and contact binaries. This is based upon the Roche model, which models each star in the system as a volume centered on the systems center of mass. Each of these lobes define the upper limit of volume that the star can occupy. Systems where both stars are entirely contained within their Roche lobe are considered detached. A system where one star fills its Roche lobe and the other is within it are considered semi-detached. Finally, systems where both stars fill or even overflow their Roche lobe are considered contact binary systems. (Hilditch 2001) W Ursae Majoris binaries are a type of contact binary, typically having short periods typically less than 0.7 days. The progenitors to these binaries are cool detached binaries that lose angular momentum due to magnetic braking, becoming contact binaries. (Stkepien 2011) The two stars in the system are typically F, G, or K stars. (Csizmadia & Klagyivik 2004) These systems have two sub types, the first being W-type where the brighter and more massive companion is the cooler star. The other is A-type, where the brighter and more massive star is the hotter star. (Binnendijk 1970)

TZ Boo, OU Ser, and CC Com are W UMa systems studied by Yakut & Eggleton (2005). TZ Boo is an A type, while OU Ser and CC Com are both W types. (Yakut & Eggleton 2005) This data set measured the period in days, along with several other physical parameters. These three objects were selected due to their very short period. Due to limited observing time, targets with short periods were absolutely essential. It is worth noting that the original paper was also able to collect spectroscopic data on each of these systems. This allowed for analysis of other physical characteristics such as individual masses, temperatures, and radii. Since our study was limited only to photometric data, these measurements were not possible. The objective of this study was to measure the period of each system using photometric data in the V passband. We will attempt to see if the period of any of the objects in question is different from the known values.

Corresponding author: Thomas Sweeney
tws13@uw.edu

This paper will first describe the observation process, then describe the methods of image reduction. Then the techniques of flux calculation and light curve creation will be described. Next there will be a comparison between the determined periods and the documented periods by Yakut & Eggleton (2005). Finally, there will be a discussion of the limitations of this work and how it could be improved in the future.

2. OBSERVATIONS

The data collected was done remotely using the ARCSAT 0.5 m telescope. This telescope is located at Apache Point Observatory in Sunspot New Mexico. The camera in use was BYUCam. Data was collected in the V passband. The targets along with their right ascension and declination in the J2000 coordinate system can be found in Table 1.

Object	Right Ascension (Hours)	Declination (Degrees)
TZ Boo	15.13587087	+39.9702398
OU Ser	15.37872222	+16.2613149
CC Com	12.20167719	+22.5329675

Table 1. Right ascension in hours and declination in degrees of target objects in the J2000 coordinate system.

2.1. *April 23, 2023*

This project had three attempts at observing runs. The first was on the night of April 23, 2023. The moon illumination that night was 10.1%. At the beginning of the observation there was a light cloud cover and high dust count, so the dome could not be opened. During this time seven bias frames were collected to be used for data reduction. Next, six dome flats were taken, three in the V and B passbands respectively. Dome flats were taken in the B passband since at that time there was consideration of observing each system in the V and B passbands. However, due to later time limitations, observations were only taken in the V band. Finally, two darks were collected with exposure times of 900 and 1800 seconds. Then after some waiting for clouds and dust to clear, an image of OU Ser was taken. This image was a 60 second exposure in the V passband. However, upon inspection in SAOImage DS9 (Joye & Mandel 2003) afterwards, it was observed that OU Ser was overexposed in the image. Unfortunately, before a shorter exposure could be taken the clouds returned and ended the observing night.

2.2. *May 3, 2023*

The next attempt at observation was on the night of May 3, 2023. Unfortunately, the moon had become much brighter, now with an illumination 93.5%. However, this was not the most pressing issue of the night, as there was a solid cloud cover over Apache Point Observatory. So the observation was canceled with no data being collected.

2.3. *May 4, 2023*

The final observing night was on the night of May 4, 2023. Thankfully, the weather that night was very clear skies. Being only one day after the previous attempt the moon was still very illuminated, at 97.7%. Importantly, there was a large angular separation between our targets and the moon. Data collection began with 15 second exposures of each of the three targets in the V band. The original plan was to take V and B band measurements of each star. Due to the time limitations imposed by the weather, this was changed. It was decided that only V band measurements would be taken. Each file was inspected carefully afterwards in SAOImage DS9 to check for over exposures. The second image collected of OU Ser was quickly recognized as overexposed. Observations then continued through the cycle, eventually returning on OU Ser with another 15 second exposure. This image was once again overexposed. At this time, it was decided that no more data of OU Ser would be collected. This was decided because there was not much time left in the observing run. In order to collect data on OU Ser, an appropriate exposure time would need to be determined, and then multiple data points taken. This would have used up too much time, which was better spent taking more data on CC Com and TZ Boo. From this point on we switched off between taking exposures of TZ Boo and CC Com.

Shortly after this, ARCSAT began having some technical issues. During exposures, the cooler would spontaneously turn off. This would cause the exposure to need to be canceled. At first turning on the cooler again allowed for the exposure to be restarted. However, this did not work later, requiring assistance from the 3.5m observer. A full restart of ARCSAT initially helped, allowing for one more image to be collected. Then the same cooler issue persisted, requiring

several restarts of ARCSAT. Eventually, it was decided that the issue could not be resolved, and the remaining hour of observation needed to be canceled. At the end of the night seven useful science images were collected. All of these images were 15 second exposures in the V band. Three were of CC Com, while the remaining four were of TZ Boo.

3. DATA REDUCTION AND ANALYSIS

3.1. *Reduction Methods*

This section will show the process for reducing each science image that was taken. Before reduction began, each image was visually inspected with SAOImage DS9 (Joye & Mandel 2003). For the images of OU Ser that were overexposed, an accurate flux reading would be unable to be achieved. There was only one non overexposed image of OU Ser, which is not enough data to fit any curve to. So, the goal of determining its period was not possible. For this reason, the images of OU Ser were not included in the data reduction process that follows.

3.1.1. *Biases*

Once all of the data was collected, each of the science images needed to be reduced to remove instrumental effects. This was done primarily with the astropy package ccdproc. (Craig et al. 2017) The first step was to collect the seven bias frames collected and combine them into one master bias. This was done using the ccdproc combine function. It is useful to use a combined bias like this since it will account for more instrumental effects in the science images. Not every bias will capture the same instrumental effects, so combining several images creates more complete image reduction. It is also important to note that ARCSAT has no over scan region on its images, so there is no need to account for them in the reduction.

3.1.2. *Darks*

The next step then was to account for dark current. Dark current is a set of pixel counts that are caused by thermal effects in the charge-coupled device (CCD), and not by the science image. So we want to remove its effect to analyze an image as unchanged by CCD effects as possible. To accomplish this, similarly to the master bias, a master dark was created. This was done by downloading other 900 second darks collected by other groups using ARCSAT. A total of four darks were to be combined into one master dark. It is worth noting that the 1800 second dark taken on April 23rd was not used here, as the master dark was created using darks of the same exposure time. Before the master dark was created, the bias was subtracted from each of the dark images. The bias subtraction was done using the subtract bias ccdproc function. This was done because the master dark will eventually need to be scaled down from 900 seconds, to the 15 seconds of the exposures of the science images. In order to scale the dark images, the bias needed to be removed since the bias is not a time dependent effect. Once the biases were removed, the combination was done using the ccdproc combine function. Similar to the biases, it is important to combine multiple darks for reduction to find all possible instrumental effects. Not every instrumental imperfection will be present in each individual dark.

3.1.3. *Flats*

Finally, a combined flat needed to be created. Before doing so, the master bias and master dark was subtracted from each V band flat. This was done with the ccdproc subtract bias and subtract dark functions respectively. When the dark was subtracted from each flat it was scaled to the same exposure time of the flat. Note that the B flats that were taken were not reduced since no science images were taken in the B band. After each flat was reduced they were combined using the combine function in ccdproc. Once again, similarly to the biases and darks, the use of several flats will decrease overall instrumental effects.

3.1.4. *Science Image Reduction*

At this point all of the calibration masters were done being created. For each image the master bias, master dark, and master flat were subtracted in that order. This was done using the ccdproc functions subtract bias, subtract dark, and flat correct respectively. The scaling of the dark exposure time was accounted for by the ccdproc function for subtracting the dark. This left us with seven fully reduced images. Three of these images were of CC Com, and the remaining four were of TZ Boo.

3.2. *Aperture Photometry*

At this point all seven of the science images were completely reduced. The next step in data reduction was to perform photometry on each image. Several methods were tried on each image to find the best result.

3.2.1. *Circular Apertures with Global Sky Subtraction*

The first method of photometry performed was circular aperture photometry. This method was used using tools from the photutils package. (Bradley et al. 2022) The first step was to perform a simple sky subtraction. This is needed since the sky glows in a fairly uniform fashion and adds a background flux value to all of the pixels in the image. Since the objective of this project is to construct a light curve, we want to isolate the flux of just the star by subtracting the background. This was done by taking the median of the pixel values in the image, and subtracting it out from the data. The median was chosen as it is less affected by the bright outlier pixels of the brightest stars in the image. So, once the sky background had been subtracted, it was possible to create the apertures. The locations of the apertures were generated using the DAOStarFinder function in photutils. This function is based on the DAOFIND algorithm Stetson (1987). Then, the radius of the apertures was chosen by zooming in on the image and fitting the edge of the aperture to the edge of the star in question. This was determined to be a radius of 50 pixels for our analysis. Finally, the aperture photometry function was run with the selected apertures, and the resulting flux of the object of interest was saved to a table.

3.2.2. *Annulus Apertures*

The next method of photometry is a small but important iteration on the previous. In the previous analysis there was a median of the entire sky taken and subtracted out. This is mostly accurate, but the local background around each star in the image will be slightly different. This means that the global background value being subtracted is not perfectly representative. Especially for the large angular area captured by our images, which sees dozens more stars than the system being studied. So to improve this method we created larger apertures that are concentric with our original aperture. Two larger circles are created with twice and triple the original radius respectively. We then found the flux through the two outer circles, and found its mean value. This value represents the local background, and was then subtracted from the flux value through their respective aperture. Similarly to before, the aperture photometry function was run with the selected apertures, and the resulting flux of the object of interest was saved to a table.

3.2.3. *Aperture methods comparison*

The differences in the background subtraction methods is slight. The method that was decided to be used for the light curve creation is using the annulus apertures for local background subtraction. This is due to the large angular area of the images taken by BYUCam. Having a field of view of 31.1 square arc minutes, many irrelevant bright stars were captured in each image. This would cause the global background to be a higher flux value than the local background. To achieve the most accurate amount of flux from just our system, local background subtraction was used. From this point forward when the flux values are mentioned, it is in reference to the flux calculated with local background subtraction.

4. RESULTS

4.1. *Flux values*

The resulting flux values from the annulus aperture photometry, along with the Julian date of the image being taken can be seen in Table 2 for TZ Boo, and Table 3 for CC Com.

Object	Image Number	Annulus Aperture Flux (adu)	Julian Date
TZ Boo	1	170976.33	2460069.6512
TZ Boo	2	187156.67	2460069.6709
TZ Boo	3	193952.87	2460069.6901
TZ Boo	4	169116.52	2460069.7316

Table 2. Flux values of TZ Boo along with their respective Julian date. The flux values do not appear linear with time.

The flux values were then normalized and plotted against time in Figure 1. It can be seen that for TZ Boo, the flux initially increases, before decreasing drastically in the last data point. This increase and decrease does not appear linear with time. For CC Com, the flux decreases at a nonlinear rate. The next logical step was to attempt to fit a curve to each of the data sets.

Object	Image Number	Annulus Aperture Flux (adu)	Julian Date
CC Com	1	91090.17	2460069.6582
CC Com	2	86900.09	2460069.6771
CC Com	3	49957.17	2460069.7071

Table 3. Flux values of CC Com along with their respective Julian date. The flux values do not appear linear with time.

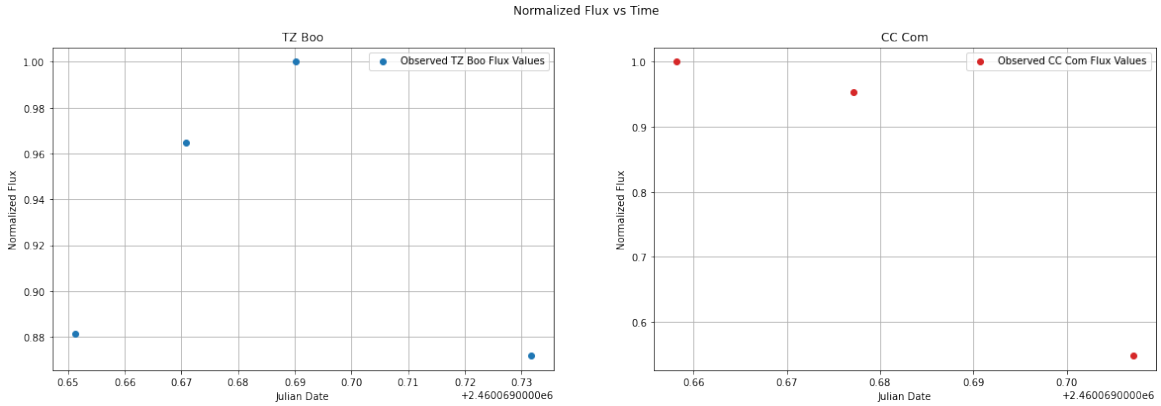

Figure 1. Normalized flux from each image plotted at their capture time. Neither data set suggests a linear relationship between flux and time. Data from TZ Boo can be seen on the left, and CC Com on the right.

4.2. *Period Determination*

Once the flux values for each of the images was determined, a light curve could be created. Upon inspection it was clear that there is not a sufficient amount of data to fit a full sinusoidal function. This is because the data points do not demonstrate the full minimum and maximum of the light curves. Also, all of the data points are within one period of oscillation. A polynomial fit was more appropriate for the small data set. The set was not observed to have a linear relationship between flux and time, as can be seen in Figure 1, so a quadratic relationship was chosen. This can also be seen by reading off the flux values from Tables 2 and 3. A quadratic of the form Equation 1 was used to fit both of the data sets. This was done using the Scipy optimize sub-package (Virtanen et al. 2020), specifically the curve fit function. The resulting fits can be seen on top of each data set in Figure 2.

$$f(t) = 1 - \frac{(2\pi f t)^2}{2!} \tag{1}$$

To obtain a period from this data, the coefficient of the second term in 1 is set equal to the determined value of this coefficient from the fit, refereed to as c. The curve fit function outputs this coefficient directly. This can be seen in Equation 2. Then by solving Equation 2 for f and inverting it, the period is determined. To determine a full light curve, all that needs to be done is to use this determined value of f in Equation 3. This will result in a full sinusoidal light curve. The substitution made in Equation 3 is valid since this represents the second order Taylor expansion. The reason that the function was mapped to cosine instead of sine is the Taylor expansion of cosine has a quadratic term, while sine does not. So it was appropriate to map the function to cosine since a quadratic fit was best.

$$c = \frac{(2\pi f)^2}{2!} \tag{2}$$

$$1 - \frac{(2\pi f t)^2}{2!} \approx cos(2\pi f t) \tag{3}$$

Before creating the light curve, the quality of the quadratic fit was assessed. This was done using the odr quadratic function in scipy. This function allowed for an assessment of how well the points fit the regression line. The results of using this function are seen in Table 4.

The quantity of residual variance tells us how well the data is fit to the regression model. The lower the residual variance, the better the fit. It can be clearly seen that both fits are good, but the fit for CC Com is exceptional.

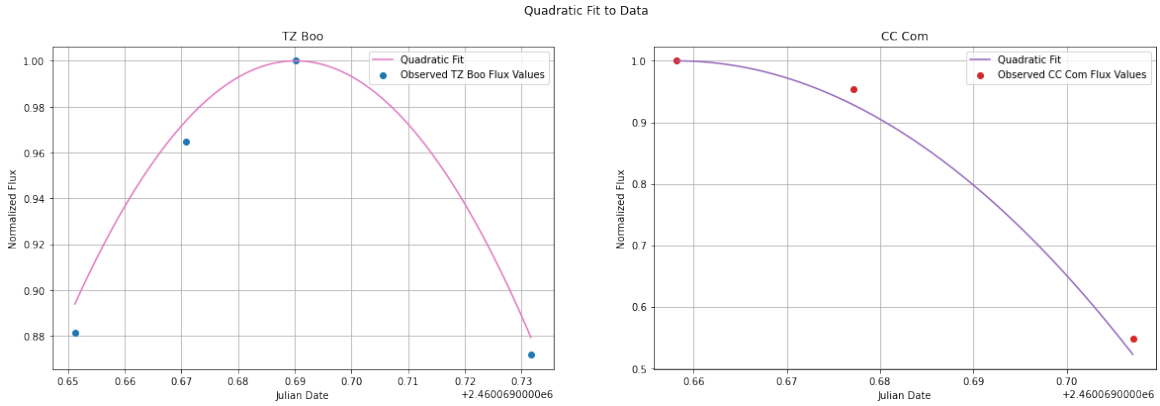

Figure 2. The quadratic fits to each data sets plotted along with the data. The quadratic is clearly a strong fit for both data sets. The fit for TZ Boo is seen on the left, while the fit for CC Com is seen on the right.

Object	Residual Variance
TZ Boo	1.570×10^{-6}
CC Com	1.659×10^{-28}

Table 4. Residual variance of each quadratic fit to the data set

4.3. *Light Curve Creation*

The periods determined using the methods found in Section 4.2 can be found in Table 5.

Object	Fit Period (d)
TZ Boo	0.5129
CC Com	0.2950

Table 5. Determined Periods for each object. These were determined from the methods described in Section 4.2

Now with the fit periods of each light curve determined, a function to plot the light curve was needed. It was decided to plot the light curves in terms of the sine function. This is an acceptable substitution to make, since sine and cosine are the same function with a different phase. So as long as the phase is accounted for, this substitution is perfectly okay. The function to plot the determined light curves with can be seen in Equation 4.

$$f(t) = \frac{1}{2} sin(2\pi f(\delta + t)) + 1 \tag{4}$$

The multiplication of $\frac{1}{2}$ and addition of 1 are simply normalization factors which do not affect the period of the function. The δ term represents an overall phase shift of the function. The quadratic fit was made to have its maximum be at the maximum flux value. For our overall light curve, we preserve this by finding the correct value of δ such that this is true. To determine the phase shift corresponding to the first maxima, the derivative of Equation 4 can be taken and set to zero, seen in Equation 5.

$$\frac{df}{dt} = \frac{2\pi f}{2} cos(2\pi f(\delta + t)) = 0 \tag{5}$$

Equation 5 is satisfied when equation 6 is true.

$$\frac{1}{4f} - t_m = \delta \tag{6}$$

Where t_m is the Julian date corresponding to the maximum flux value. Note there are infinite values that will satisfy Equation 5, but the solution in Equation 6 will give the first maxima available. Once the correct δ for each curve is determined, it can be plugged into Equation 4 and plotted to see the full light curve.

4.4. *Light Curve Results*

The light curves generated using the methods in Section 4.3 can be seen in Figure 3. The associated periods determined by this method can be seen in Table 5.

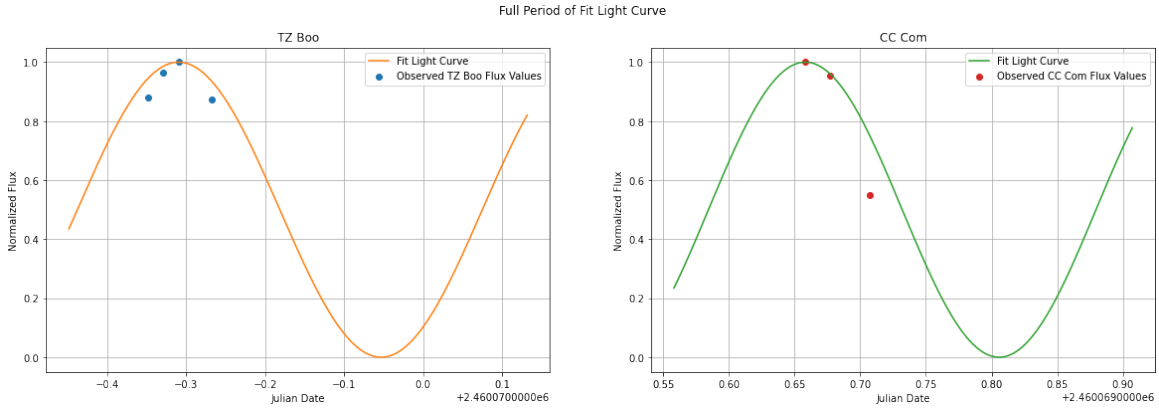

Figure 3. A full period of each light curve generated using the Taylor approximation method. The original data is found surrounding the first maximum for both curves. The curve for TZ Boo is seen on the left and the curve for CC Com is seen on the left.

4.5. *Quadratic vs Full Fit*

The difference in the fit of the quadratic function and cosine can be seen in Figure 4

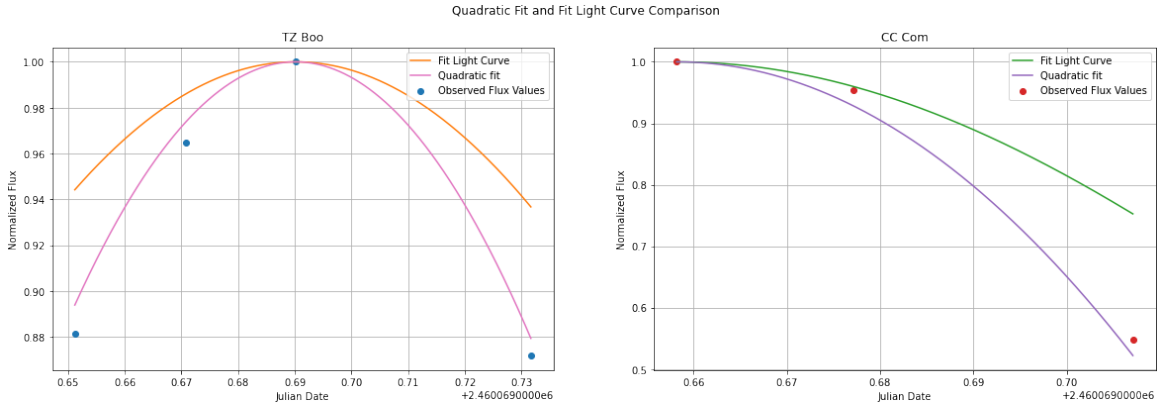

Figure 4. A close up of each objects data points, quadratic fit, and fit light curve. It can be seen that for both, the fit light curve over estimates the data points. The data for TZ Boo is seen on the left, and CC Com on the Right.

It appears that the fit light curve and quadratic fit look a bit different near the data. This can be easily explained by the qualities of the Taylor series expansion. The second order approximation of cosine with this method is inaccurate outside of a small range where the parabola is a strong fit, since the Taylor series only fits functions locally. Each of the quadratic fits are only designed to fit the range of data points given. This means that the quadratic approximation to the cosine function will look different from the cosine itself. The main difference will be the width of the functions being different, seen in Figure 4. When the cosine decreases from its maximum its slope will be much lower than the quadratic. This is because the function is approaching an inflection point and will have the sign of its slope change. The quadratic will always be concave down, so it have an increasing negative slope as time moves forward. This all results in the cosine having a maximum with a much greater width than the quadratic fit. This overestimation of width will result in an overestimation of period. This is because the width being larger will mean it takes more time to complete a full cycle.

5. DISCUSSION

5.1. *Plotting known period*

Due to the periods of TZ Boo and CC Com being known, it was chosen to compare the fit light curve against the previously calculated period values in Yakut & Eggleton (2005). The values for each of the objects can be seen in Table 6

Object	Known Period (d)
TZ Boo	0.2976
CC Com	0.2210

Table 6. Period values of observed objects. These are known from Yakut & Eggleton (2005).

The natural comparison is to compare the two light curves against one another. So the plotting of the known period as a full light curve was the next objective. To create this light curve, a sinusoidal oscillation was assumed. The function was normalized along with the flux values of the data. The resulting function to plot is Equation 4. The value for delta can be determined by the same methods as described in Section 4.3 using Equation 6. Once this values were determined, they was plugged into Equation 4.

These light curves were plotted with the light curves shown in Section 4.4. This is seen for TZ Boo in Figure 5 and for CC Com in Figure 6. Each figure shows a close up of each fit around the data points, as well as a full period of oscillation for the fit curve.

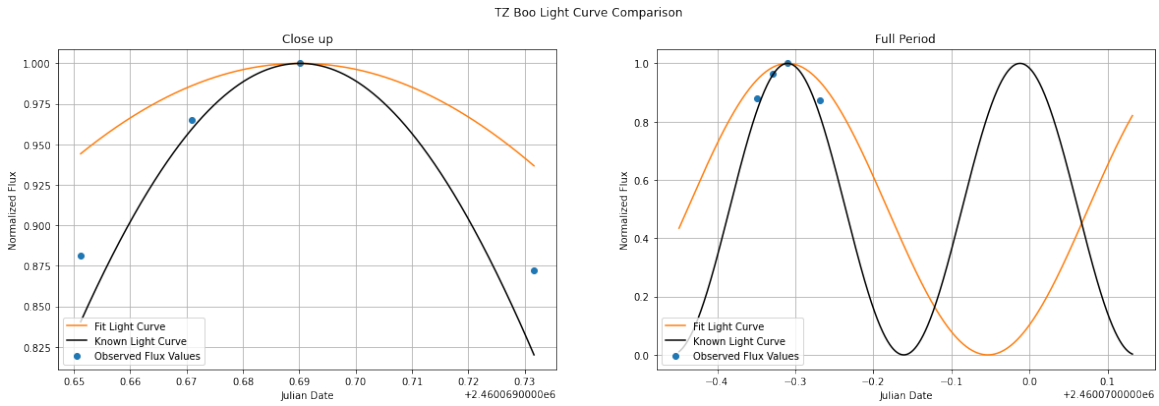

Figure 5. The fit light curve for TZ Boo from 4.4 is plotted alongside the known TZ Boo light curve. The original TZ Boo data points are also visible. The fit light curve appears to overestimate the period of the data. A close up can be seen on the left, while a zoomed out full period can be seen on the right.

Object	Fit Period (d)	Known Period (d)	Percent Error
TZ Boo	0.5129	0.2976	72.33%
CC Com	0.2950	0.2210	33.47%

Table 7. Determined and Known Periods for each object with respective percent error

5.2. *Period Data discussion*

As can be seen in Table 7 both of the determined periods are overestimates of the known period values. This overestimation is exactly what was predicted in Section 4.5. The percent errors of the periods are fairly high, but are within the correct order of magnitude. The limitations of the data being in one part of the period make it impossible to model with anything but a quadratic. Visually, the known period does appear to be a much better fit of the data compared to the fit period.

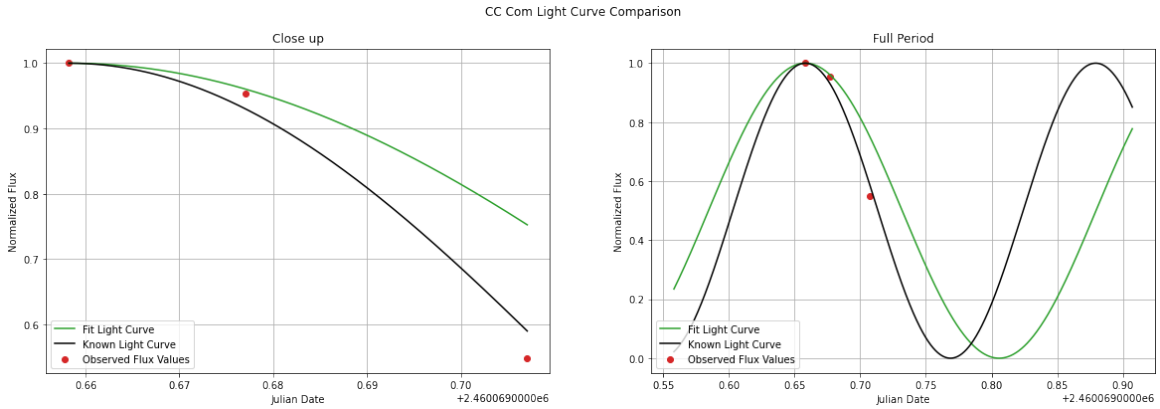

Figure 6. The fit light curve for CC Com from 4.4 is plotted alongside the known CC Com light curve. The original CC Com data points are also visible. The fit light curve appears to slightly overestimate the period of the data. A close up can be seen on the left, while a zoomed out full period can be seen on the right.

It is worth noting that CC Com has about half of the percent error of TZ Boo despite having one less data point. This could be for many reasons, one being the randomness of data collection. It is possible that the data collected of CC Com is very similar to the data collected by Yakut & Eggleton (2005). While for TZ Boo, it is possible that the first and last data points were taken at points where more star spots were visible. This would have caused a higher flux reading than what is expected by the known light curve at those times. However, the far more likely explanation is that the original quadratic fit for the data was much better for CC Com compared to TZ Boo. This can be easily seen in Table 4, where CC Com has a incredibly low residual variance. This higher quality initial fit propagated into a higher quality estimation of period. So overall, both fits had a fair amount of error, but give a reasonable estimate at the period of each system. CC Com has an overall more accurate estimate due to its superior initial fit.

5.3. *Limitations of Data Quantity*

There were many limitations that the lack of data caused. Some include uncertainty of extrema, limited options in fitting methods, and the inability to model OU Ser. These will each be explored in detail in this section.

5.3.1. *Extrema Uncertainty*

One limitation of the small data set is there is uncertainty of the true maxima of each light curve that was generated. Both the light curve created by fitting methods, an the light curve with known period were fit to have their maximum be at the maximum flux value. Due to the minimal data though there is no reason to be certain that the maximum flux measured is the true maximum. It is quite likely that the maximum flux is greater than the one measured for both objects. This is because the probability of one random data point being the global maximum is very low. If the true maximum flux was greater, then the modeled parabola would have a smaller width. This in turn would yield a smaller period value, closer to that of the known period. Thus it seems quite likely that the true maximum was not measured, due to probability and the resulting overall period. If more data was collected, the probability of measuring values closer to the true maximum would increase. This would increase the quality of the period measurement.

There is greater uncertainty with the minimum flux emitted by each system. Neither system was observed at its minimum flux, as both data sets indicate a concave down curve. This means that the measurements were all taken before the inflection point of the curve. Thus, all of the data points were taken closer to the maximum flux than the minimum flux. A lack of data near the minimum flux means that an accurate amplitude of either light curve cannot be estimated. However, due to the properties of sinusoidal functions, this does not affect the ability to estimate the period of the function. Nonetheless, it would be useful for creating a more accurate light curve to understand the minimum and by extension the amplitude of the function. Data near the minimum would also allow for increased accuracy in period estimation.

5.3.2. *Limited Fitting methods*

The main limitation of the small data sets is that only a second order polynomial could be accurately fit to the data. With a larger data set, a higher order polynomial could have been fit. As discussed in Section 4.5, the limited degree

of the fit polynomial resulted in an overestimation of period. If a higher order polynomial could be fit, then a higher order Taylor expansion could have been fit. Additional terms in this Taylor series approximation would allow for a more accurate period to have been estimated with the Taylor series method. This is because the more terms included in a Taylor expansion, the more accurate the expansion is to the function that is being approximated. This would have cause a tighter fit to the data set, and likely would produce a shorter period more in line with the actual values.

While a higher order polynomial would allow for a better approximation of a sinusoid, the ideal case would be a direct sinusoidal model of the data. This could be achieved with much more data that is spaced out. All of the data collected on both objects was within one period. If there was additional data taken from different periods, a sinusoidal model could be achieved. The Taylor series model will always just be a less accurate model of the direct function. So with more data, all of the inaccuracies of the Taylor approximation could be avoided.

5.3.3. *Assumptions of Sinusoidal Light Curve*

A large assumption that was made in the modeling of the light curves was a perfect sinusoidal oscillation. W UM a binaries have real light curves that look different than a normal sinusoid. They typically spend more time near their maximum flux, before quickly and sharply passing through their minimum flux. (Kjurkchieva et al. 2018) Due to the limited data, nothing more complicated than a normal sin curve could be approximated. However, given more data a more accurate and intricate light curve could have been determined. This does explain why both sets of data were found close to a maximum, as these systems spend much more time near their maximum flux.

5.3.4. *Issues with OU Ser*

The lack of data quantity made a period determination of OU Ser impossible. With only one valid science image, no light curve could be fit. With more observation time, an appropriate exposure time could have been calibrated. Then more data points could have been collected, and a light curve could have been constructed using the same methods as for TZ Boo and CC Com.

5.4. *Limitations of Data type*

Only photometric observations in the V band were made. This section will discuss the limitations of the filters used, as well as the overall constraints of photometric data.

5.4.1. *Filters*

All of the observations were only done in the V band. With more observation time, measurements in other filters such as the B band could have been made. The advantage of that would be a determination of spectral type and temperature. This could be done with the methods demonstrated in Moriarty (2015). Also, the B band flux could be plotted into a light curve of its own and be similarly analyzed. Then the two determined periods could be compared against one another. Overall, observations in another filter would allow for additional information about the stars within the system.

5.4.2. *Photometric Data*

There are certain limitations to what can be done with photometric data. Since all of our systems are contact binaries very far from Earth, their separation cannot be directly observed. So, in order to determine their separation, spectroscopic data is necessary. Obtaining spectroscopic data of these systems would allow for many physical parameters to be determined. For example methods similar to those used in Fekel & Willmarth (2009) could be used to determine the radial velocity and other physical parameters. These can include eccentricity, individual masses and individual radii.

6. CONCLUSION

The objective of this project was to determine the periods of the three systems of interest. For the systems TZ Boo and CC Com the periods were able to be determined, while for OU Ser the period was not able to be determined.

Though data collection was plagued by bad weather, data reduction and photometry went incredibly successfully. The methods for turning observation into data suitable for modeling curves have been streamlined. In the future if more data collection is possible, the data reduction pipeline is entirely prepped.

The creation of light curves and determination of period was successful, but prone to large amounts of error. With additional data collection in the future, the models created could be exponentially improved. Overall, the determination of a period within the correct order of magnitude with such a limited data set is in some sense a success.

Aside from additional data points the main improvements for the future include data taken in more wavelength ranges. This would allow for confirmation of the spectral class of the stars in each system. Also, spectroscopic data on these systems would allow for measurement of many other physical parameters. This would allow for a more detailed study of the evolution of each system. For example, spectroscopic data would allow for calculation of the mass ratio. This ratio could be compared against the values determined in Yakut & Eggleton (2005). This would allow for study of the mass transfer ratio between stars and how that contributes to their evolution.

Overall, this project was a successful start to understanding TZ Boo and CC Com, and will hopefully lead to further understanding of them in the future.

REFERENCES

Binnendijk, L. 1970, Vistas in Astronomy, 12, 217, doi: 10.1016/0083-6656(70)90041-3

Bradley, L., Sipőcz, B., Robitaille, T., et al. 2022, astropy/photutils: 1.5.0, 1.5.0, Zenodo, doi: 10.5281/zenodo.6825092

Carroll, B. W., & Ostlie, D. A. 2017, An introduction to modern astrophysics, Second Edition

Craig, M., Crawford, S., Seifert, M., et al. 2017, astropy/ccdproc: v1.3.0.post1, doi: 10.5281/zenodo.1069648

Csizmadia, S., & Klagyivik, P. 2004, A&A, 426, 1001, doi: 10.1051/0004-6361:20040430

Fekel, F. C., & Willmarth, D. W. 2009, PASP, 121, 1359, doi: 10.1086/649047

Hilditch, R. W. 2001, An Introduction to Close Binary Stars

Joye, W. A., & Mandel, E. 2003, in Astronomical Society of the Pacific Conference Series, Vol. 295, Astronomical Data Analysis Software and Systems XII, ed. H. E. Payne, R. I. Jedrzejewski, & R. N. Hook, 489

Kjurkchieva, D. P., Popov, V. A., Vasileva, D. L., & Petrov, N. I. 2018, NewA, 62, 46, doi: 10.1016/j.newast.2018.01.008

Moriarty, D. J. W. 2015, JAAVSO, 43, 151

Stetson, P. B. 1987, PASP, 99, 191, doi: 10.1086/131977

Stkepien, K. 2011, AcA, 61, 139, doi: 10.48550/arXiv.1105.2645

Virtanen, P., Gommers, R., Oliphant, T. E., et al. 2020, Nature Methods, 17, 261, doi: 10.1038/s41592-019-0686-2

Yakut, K., & Eggleton, P. P. 2005, ApJ, 629, 1055, doi: 10.1086/431300

ACKNOWLEDGEMENTS

Huge thank you to Professor Tuttle and Steven Stetzler for being an amazing instructor and TA! The constant encouragement kept me going through this project and I cannot thank you enough.

My co-authors and other classmates were integral in the development of this work and I truly appreciate the feedback they provided me.

This research has made use of the SIMBAD database, operated at CDS, Strasbourg, France

Lots of thanks to Matt Craig and Lauren Chambers, and all the other contributors to the CCD Data reduction guide! It was essential in my data reduction process.

Finally, a gigantic thank you to my amazing family members, Mom, Dad, Elizabeth, and Jack. As well as my wonderful girlfriend Molly, for consistently listening to me talk about this paper and giving me endless support for the past few months. I hope you thought the graphs looked pretty!